Pho Van NGUYEN [1,2], Phi N. NGUYEN[2], Tan NGUYEN[2],
Thanh Lanh LE[2]

Hybrid robot hand for stably manipulating one group objects

Autonomous manipulation of group objects requires the gripper/robot hand to achieve high productivity without poor outcomes such as object slippage and damage. This article develops the robot hand capable of achieving effective performance in each trial of grasping the group objects. Our proposed robot hand consists of two symmetrical groups of hybrid fingers having soft pads on the grasping interfaces, which operate as a comb. The grasping ability of this robot hand was theoretically and experimentally validated by handling three groups of objects showcases: tea packs, toothbrushes, and mixing sticks. Additionally, validation results were compared with those of another soft robot hand having soft Pneunet fingers. In each trial, the experimental results showed that the proposed robot hand with hybrid fingers achieved more stable grasping states characterized by a higher number of grasped objects than those in the case of the soft robot hand. Also, experimental results were in good agreement with the predictions of the proposed theoretical analysis. Finally, better performances of the hybrid robot hand in handling the group object provide the bases for developing a novel-robotic application in industrial production.

1. Introduction

Nowadays, the need of applying autonomous manipulation to production lines is more and more emergent, especially in handling soft fragile objects. Such kinds of objects require the robot hand to generate soft-friendly interaction during handling

✉ Pho Van Nguyen, email: ngvphobk08@gmail.com

[1]Japan Advanced Institute of Science and Technology, 1-1 Asahidai, Nomi, Ishikawa, Japan; ORCID: 0000-0002-7794-7863

[2]Department of Technology, Dong Nai Technology University, Bien Hoa 810000, Vietnam

for avoiding poor outcomes. Hence, this study aims at finding an appropriate method for a robot hand in handling a large number of objects in an efficient-productive way. From the given scenario, one gripper/robot hand can increase its manipulation for one grasped object in each grasping trial by varying operation velocity. However, this way becomes ineffective for the huge number of grasped objects. More feasibly, the robotic gripper can grasp a greater number of objects in each grasping trial instead of only one. Hence, we investigate the mechanisms in both soft and traditional robotics to develop a novel robot hand that can stably manipulate a group of soft delicate objects per grasping trial.

Manipulating one object at each grasping time in robotic applications was presented in soft robotics [1, 2]. Due to the soft properties of the soft body, the soft robot hands can create soft-friendly interactions with their contact environments. Among them, a patterned polymer mimicking the dry adhesive leg of a gecko was helpful for a Stickybot to climb walls [3] and as a gripper to handle dry objects [4]. Shintake [5] reported a gripper actuated by a dielectric elastomer to create electro-adhesion force between the gripper and the grasped object. Grasping objects by a suction cup attached to an octopus robot arm [6] had an advantage in speed manipulation. Another soft gripper presented in [7–12] can manipulate several soft objects such as food samples. These principles were appropriate for robotic manipulation in dry conditions, whereas an octopus-like robot arm [13] and a soft gripper [14] could handle large objects under water. However, the studies on manipulating group objects at each trial have not yet been mentioned in soft robotics. Compared with the soft robotic hands/grippers mentioned above, the conventional robotic grippers in [15] may perform more stably in gripping and holding the group objects due to their rigid fingers. However, the rigid gripper can damage the object's attributes such as surface and body shape by the hard interaction. Furthermore, also the studies on autonomously manipulating the group objects are still scarce in the traditional robotics. In forestry, the cranes in [16, 17] can grip the bars of wood under the control and supervision of a driver and other workers. Nevertheless, such a crane is hard to apply to autonomously handle a soft delicate object in high safety conditions.

This paper firstly modelled a theoretical analysis to explore the mechanics of grasping one group of soft-delicate objects. Then, we proposed a novel hybrid robot hand for conducting the manipulating evaluation that was compared with the case of the soft robot hand. Our study has made the following contributions:

1. Building an analytical model for estimating the kinetics in grasping the group objects. This model can be a useful platform for other researchers.
2. Designing the hybrid robot hand for effectively grasping the group objects.
3. Comparing the ability of the hybrid and the soft robot hands in grasping different object's showcases.

In this paper, section 2 illustrates analytical models of grasping group objects. Section 3 shows the design of robot hands in handling the group objects. The next section presents the fabrication of the robot hands designed in section 4 and

the conducted experiments. The results in section 5 include comparisons between hybrid and soft robot hands in terms of ability of grasping the group objects. Section 6 contains a discussion about the key problems of the analytical model described in section 2 and experiment results in section 5. The final section presents conclusion and work suggested for future improvement.

2. Kinetics of grasping multiple objects

As shown in Fig. 1a, there are n identical objects lying on the floor and having length l_o, and cross section area A_o. At the initial state, the objects lay closely together in a uniform way. A robotic hand having two symmetrically fingers is assembled on the end of a 6-DOFs robot arm, which can generate translation and rotation movements in x_r, y_r, z_r axe and φ_x, φ_y, φ_z directions. In the global coordinate system, two robot fingers are separated with a gap y_{ti} and a height z_{ti} from the highest point of the objects. Before the robot hand contacts the objects, each object interacts with its neighbor objects, which causes that the appearance of
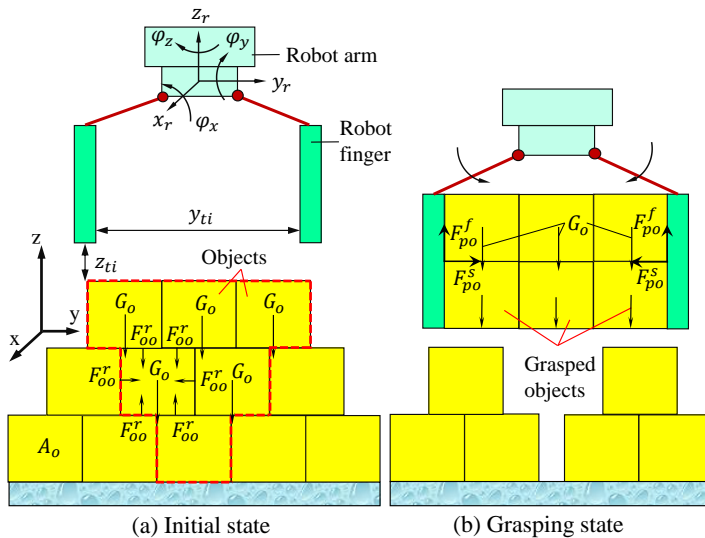

Fig. 1. Illustration of manipulating one group object per a grasping time by the 6-DOFs robot hand. (a) Initially, the hand opens its fingers with a distance y_{ti}, and the lowest point of the fingertips takes a position above the highest point of group objects lying on the floor. The red-dash curve is the border that separates the regions where the group objects are grasped, or will be grasped in the next step. F_{oo}^r, G_o are the reaction force acting on one object with its neighbors, and the gravity force acting on one object. In v the initial state of our research, for the sake of simplicity, we assumed that the objects are identical and have a square cross section. (b) Then, the robots' hand moves down along z-axis to penetrate the group objects, closes its finger inward and grasps a number of the objects. The forces generated by the robot fingers acting on the group of grasped objects in this picture are squeezing and friction forces, F_{po}^s, F_{po}^f, respectively. After that, the robotic hand holds a number of objects and moves up during the lifting phase

the resultant force F_{oo}^r appears at the contact interfaces (see Fig. 1a). Also, at the contact surfaces, there are other forces, which can restrict the motion of the objects such as adhesion, friction and the interlock force [18]. Also, the gravity force G_o acting on each object generates the compression load increasing from the top to the bottom layers [19]. Due to the effect of G_o the objects become more closely interconnected. For an arbitrary object j in Fig. 1a, the total force acting on it can be calculated as follows:

$$\overrightarrow{F_o} = \overrightarrow{G_o} + \sum(\overrightarrow{F_{oo}^r} + \overrightarrow{F_{oo}^f} + \overrightarrow{F_{oo}^i} + \overrightarrow{F_{oo}^a}),\tag{1}$$

where $F_{oo}^f, F_{oo}^i, F_{oo}^a$ are the friction, interlock and adhesion force [20, 21] between two objects, respectively. Depending on the object's properties such as mechanical properties, shape, and the arrangements, F_o in Eq. (1) varies per object. Indeed, the objects lying in the lower layers bear larger loads than the others in the upper layers or the outer region. Additionally, in Eq. (1), the gravity direction is along z axis, whereas the directions of the remaining forces depend on the contact surfaces.

Let us assume that there are m objects inside the red-dashed line region at the initial state (see Fig. 1a) grasped by the robot hand at one time. Then, these objects are grasped and lifted in a group inside the space between two fingertip sides (see Fig. 1b). Now, applying equation (1) to the case of the group having m objects we derive the total force that equals to the right hand side of Eq. (2):

$$\overrightarrow{F_o^g}|_m = \{\overrightarrow{G_o} + \Sigma(\overrightarrow{F_{oo}^r} + \overrightarrow{F_{oo}^f} + \overrightarrow{F_{oo}^i} + \overrightarrow{F_{oo}^a})\}|_m.\tag{2}$$

The robot hand gradually moves down to separate the objects into two regions: the *grasped objects* – inside the red-dashed curve and the *remained objects* – outside the red-dashed curve (see Fig. 1a). Then, it pushes the fingers toward each other group for grasping and lifting the objects from the groups. Before the objects are grasped and lifted, we can consider that the objects are in a stable state or there is no motion within the group. Hence, the force $F_o^g|_m$ can be assumed approximately constant in each phase. To carry out the grasping, the robot hand must generate a squeezing force on the surfaces of contact between the objects F_{po}^s. Thanks to this force, the friction force is created for reducing possibility of slip between the robot fingers and the objects F_{po}^f. According to [22], the friction force can be estimated as a product proportional to the squeezing force, so we have $F_{po}^f = \mu F_{po}^s$. Hence, the robot hand successfully grasps the object when the following condition is satisfied:

$$F_{po}^s \geq \frac{F_o^g|_m}{1 + \mu}.\tag{3}$$

In Eq. (3), $F_o^g|_m$ can be estimated in Eq. (2). Determining the inequality Eq. (3) for the coordinate axes allows for deriving the minimum required value of F_{po}^s. In addition, Eq. (3) shows that the robot hand needs sufficient squeezing and friction forces for obtaining a successful grasp.

3. Design of robot hand

Based on the analytical model in section 2, this section shows our design of the robot hand for safely handling one group of objects at each grasping time. Since the robot design aims at effectively grasping various types of the objects, we assume that the objects may be in intertwined. In this scenario, the designed robot hand must successfully creep into the area before taking the grasping pose. Hence, the design of robot hand having multiple fingers is a more suitable option. Besides, in order to assure stable grasping, we also consider the soft handling for the safety of the object surfaces during grasping. There are two design options: the hybrid fingers and the soft fingers.

3.1. Design of robot hand with hybrid fingers – hybrid robot hand

In the hybrid robot hand in Fig. 2, there are two opposite sides having five rigid fingers at each side. The fingers at each side, which are synchronously rotated by two connected rods, are driven at the four finger ends by the gear transmission consisting of front and rear gears. The front gear at the right hand side is fixed to a rotation shaft of a servo motor. Also, the finger has a curved shape in order to increase the number of grasped objects. A soft pad is attached to the contact surface of the robot finger for ensuring soft interactions between it and the object's surfaces during gripping. The hybrid fingers are positioned as two teeth of a comb. The finger's gear is assembled with the motor's shaft, then this system is fixed on the robot body before attaching it to the robot arm by the connector part (see Fig. 2b). The motor controls the grasping and releasing operations of the hybrid robot hand

(a) Design of
hybrid robot hand

(b) Actual application in
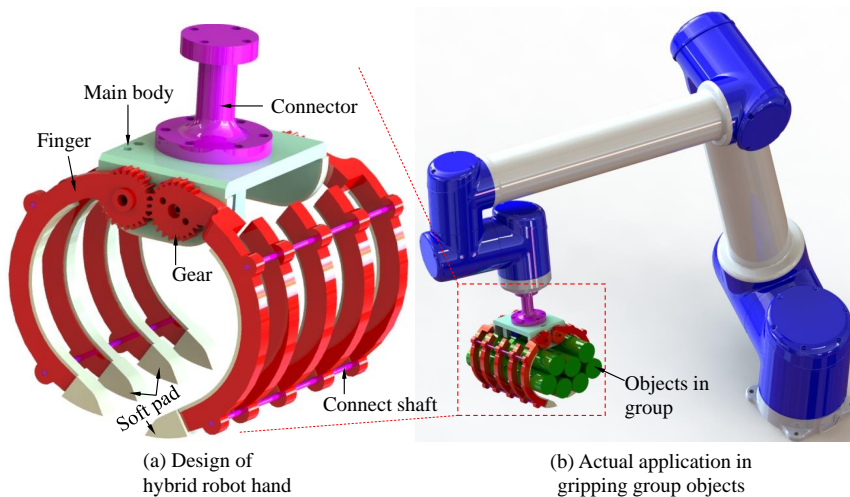gripping group objects

Fig. 2. Design of the hybrid robot hand for grasping one group of the objects. (a) The assembly design of the hybrid robotic hand. (b) Fixing the robot hand on the robot arm. In this picture, the hand holds one group of objects between the fingers

through the rotation of fingers. In addition, the gears are designed so that they have a large number of teeth and a big module to ensure good intermeshing. Hence, the vibration during grasping of the objects is reduced.

3.2. Design of robot hand with soft fingers – soft robot hand

In this scenario, the soft robot hand (see Fig. 3) has two symmetrical sides of Pneunet fingers having the Pneunet structure, the main body, a connector, an adjustable part and a pneumatic actuator system. Each side of the soft robotic hand had three identical soft Pneunet fingers consisting of two components: the cover and the chamber skin, both made from soft materials. Such components are sealed with a silicon glue film. One end of each soft finger has a pneumatic pipe connecting it to a pneumatic system. After that, the soft fingers are placed inside the grooves of the adjustable parts, which can vary the gap between the two sides of the soft Pneunet fingers before attaching them to the robot arm through the main body and the connector. In this design, the pneumatic system controls both the grasping and releasing operations of the fingers. Also, in order to increase the friction force between the object's surface and the grasping surface of the soft fingers, the surface is textured with a straight pattern. Also, the fingertips have sharp edges and an increased stiffness to easily penetrate the objects.

(a) Design of soft
robot hand

(b) Actual application in
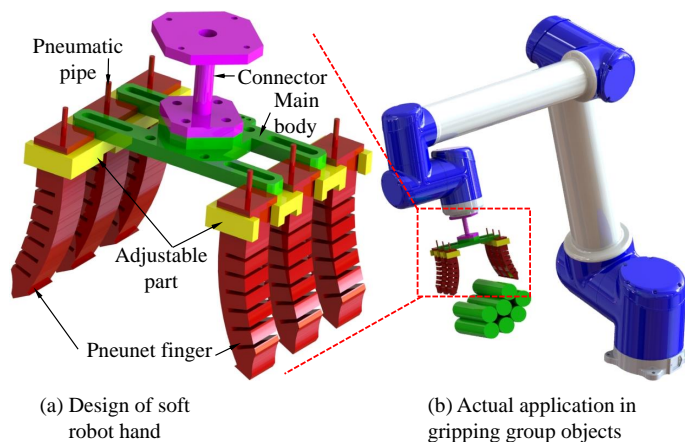gripping group objects

Fig. 3. Design of a soft pneumatic hand for manipulating one group of the objects at one time. The hand consists of the soft fingers controlled by pneumatic pressure. (a) The schematic of the soft robot hand assembly. (b) Attaching the robot hand to a 6-DOFs robot arm

4. Materials and method

Based on the design model described in the previous section, we aimed at showing the fabrication process for hybrid and soft robot hands, which would then be set up for carrying out grasping experiments. The outcome of experiments shows

comparison of grasping ability between such robot hands in handling one group objects at a time.

4.1. Fabrication process of the robot hand

4.1.1. Soft robot hand

The main body, the connector, and adjustable components of the designed soft robotic hand in Fig. 3 were created by means of a Zotrax 3D printer, meanwhile the robot fingers were made with the processes illustrated in Fig. 4. Initially, we created molds to cast the soft cover skin and the chambers, as shown in Fig. 4(a-1) and (b-1). The Dragon Skin 00-30 in liquid state mixed at the weight ratio of 1:1 was poured into the molds (Fig. 4(a-2) and (b-2)) and the air bubbles inside the liquid were removed by using a vacuum machine, as shown in Fig. 4(a-3) and (b-3). Then, the shape molds were put upon the liquid silicon rubber to form the shape of the chamber and skin, as shown in Fig. 4(a-4) and (b-4). After the silicon rubber completely turned to the solid state, we removed them from the molds and then sealed them together for creating the soft Pneunet fingers (in Fig. 4c). Also, one

(a-1) Cover mold   (b-1) Chamber mold

(a-2) Pour silicon rubber   (b-2) Pour silicon rubber

(a-3) Degas   (b-3) Degas

(a-4) Casting silicon rubber   (b-4) Casting silicon rubber

(a) Fabricate   (b) Fabricate   (c) Fabricate soft
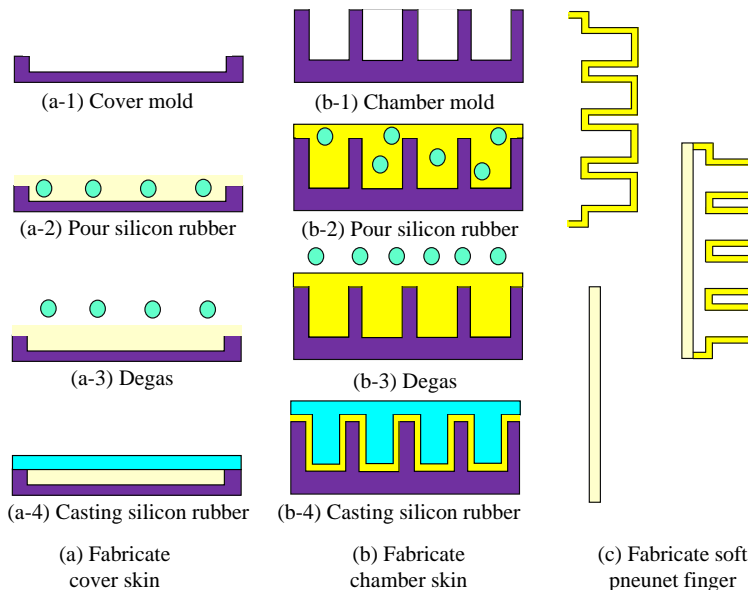cover skin   chamber skin   pneunet finger

Fig. 4. Step-by-step fabrication process of one Pneunet robotic finger. Fabrication procedure for the cover skin (a) and the chamber skin (b). The cover (a-1) and skin molds (b-1) are printed by using a 3D printer. After that, the silicon rubber in liquid state is poured to the printed molds (a-2) and (b-2). A vacuum machine is used to suck the air bubble out of the liquid silicon rubber (a-3) and (b-3). Other upper molds (blue parts) are used to create the final solid shapes of the cover (a-4), and the chamber skin (b-4). After attaining the solid state, the cover and chamber skins are removed from their initial molds and sealed together for creating the Pneunet fingers. Finally, the air leakage is tested and the whole process is duplicated for fabricating other soft fingers

end of the soft fingers was connected with a pneumatic pipe for receiving signals of the air pressure. The soft fingers were then affixed to the grooves of two adjustable parts, which were fixed to the main body and the robot hand. The maximum gap between an opposite pair of the fingertips was about 200 mm. The fabricated soft robot hand is shown in Fig. 5b.
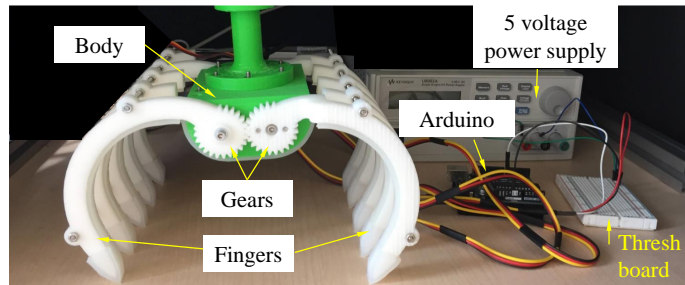
(a) Setup experiment for hybrid robot hand
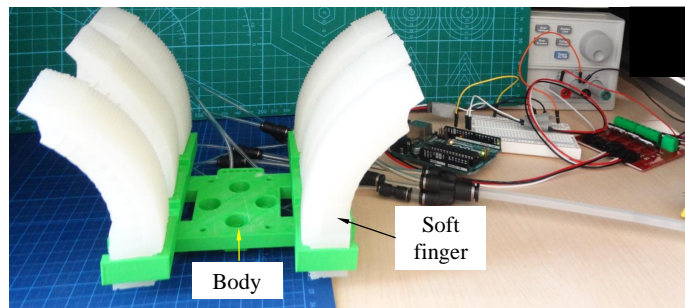
(b) Setup experiment for soft robot hand

Fig. 5. The fabricated products and experimental setting of grasping the group objects per grasping time for (a) the hybrid and (b) soft robot hands. The fabricated soft robot hand was in open state and was controlled by the pneumatic system including the Arduino, MOSFET T4, 3/2 electromagnetic valve, pressure sensor, vacuum ejector, compressor, throttle valves and network of pneumatic pipes

4.1.2. Robot hand with hybrid fingers

As illustrated in Fig. 5a, many parts of the designed hybrid robot hand in Fig. 2 were fabricated by means of a Zotrax 3D-printer at very high accuracy level. The soft pads cast from silicon rubber Dragon Skin 00-30 Smooth-on were used to cover the grasping interfaces of the hybrid fingers. Five fingers at each side were fixed with two thresh shafts M3 at two holes on the finger's body, while the four gears at the finger's ends were fabricated with a module of 1.25 mm. The driving gear was assembled with a motor type Dsservo-Coreless Digital Servo 35 kg. When the motor shaft rotated in clockwise and anticlockwise directions, the hybrid fingers opened and closed, respectively. The maximum normal gap between two opposite fingertips was 240 mm. The obtained hybrid robot hand is illustrated in Fig. 5a.

4.2. Experimental setup

4.2.1. Grasping experiment

The DS servo motor of the hybrid robot hand was supplied from a Keygen power source, and connected to a UNO Arduino, as shown in Fig. 5a. The Pneunet fingers were supplied with air pressure from a compressor and the air was sucked out through a vacuum ejector. The air flow inside the Pneunet robot fingers was controlled by a pneumatic circuit consisting of two electromagnetic 3/2 valves, Mostfet4 and the UNO Arduino, as illustrated in Fig. 5b. For this experiment, we selected three types of object samples: a mixing-stick (80 items), a toothbrush (24 items), and a tea pack (35 items) (see Table 1) laid on the floor in a random way. Initially, the robot fingers' position was such that the fingertips were 70 mm above the floor. After that, the robot hands opened to the maximum y_{ti}, moved down until the fingertips contacted the object's surfaces, and closed the fingers to grasp the objects step-by-step. Then, these robotic hands gripped and lifted up the group objects, moved down, and finally released the grasped objects. In this scenario, each kind of the experiments was carried out five times. The processes of grasping were recorded with a camera Sony HDC HX300 and the images were processed in MATLAB environment.

Table 1. Main parameters of the object showcases

Object	Weight, g	Length, mm	Width, mm	Height, mm	Stiffness
Mixing stick	11.4	205	19.7	5.29	rigid
Toothbrush	5.4	157	11.4	15.5	rigid
Tea pack	4.2	137.87	35.25	7.68	soft

4.2.2. Measuring squeezing force

One of the soft robot fingers attached to a fixed frame was in contact with the probe of a force sensor Imada 5 N in the stationary state. When the air pressure was inputted to the Pneunet chamber, the squeezing force generated by the soft robot hand $F_{po,y}^s$ was recorded at two points: the fingertip and the middle point.

5. Results

This section describes the experimental results obtained in previous sections. The experiments were aimed at comparing the ability of two kinds of the robot hand, the hybrid and the soft one, in grasping one group of objects a time.

5.1. Squeezing force

In Fig. 6a, the squeezing force $F^s_{po,y}$ at the fingertip and the middle point of the soft robot finger is proportional to the air pressure inside the chamber. In other words, this force at the middle point and the fingertip reaches maximum values of 1.8N and 1.5 N, respectively, at the maximum pressure of 40 kPa inside the finger chamber. According to the results shown in Fig. 6b,c, the fingertip has a displacement larger than that of the middle point at the same level of the air pressure inside the finger chambers. This significantly changes the contact surface of the finger. Hence, there is a big variation of the force $\overrightarrow{F^s_{po}}$ along the length of the soft robot finger.
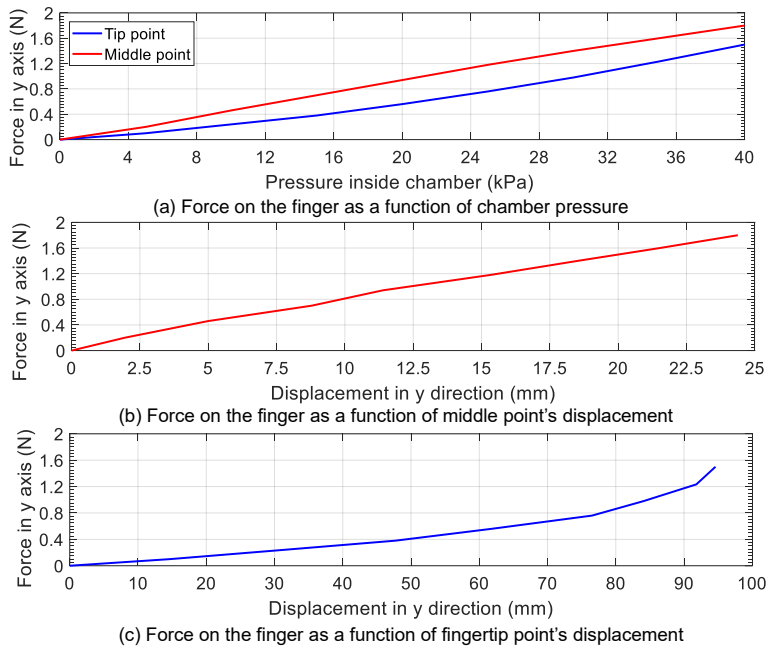
Fig. 6. Measurement of the squeezing force in *y*-direction at the fingertip and the middle point of the soft robot finger. (a) Measuring the squeezing force of the soft fingers through varying the air pressure inside the finger chamber. (b) and (c) the squeezing force acting on the soft finger versus the displacement function at the fingertip and middle point

In the case of the hybrid robot hand, we divided the hybrid finger in to five points numbered from $1 \div 5$ where $l_1, l_2, l_3, l_4, l_5, l_{cg}$ are the distances from the gear center to the points $1, 2, 3, 4, 5$ and to the centerof gravity of the finger (see Fig. 7a). According to the Newtonian law, the force generating from rotating the hybrid finger is:

$$F^s_{po} = m_f l_{cg} \frac{d^2\alpha}{d^2 t}, \tag{4}$$

(a) Distribution of squeeze force on one hybrid finger

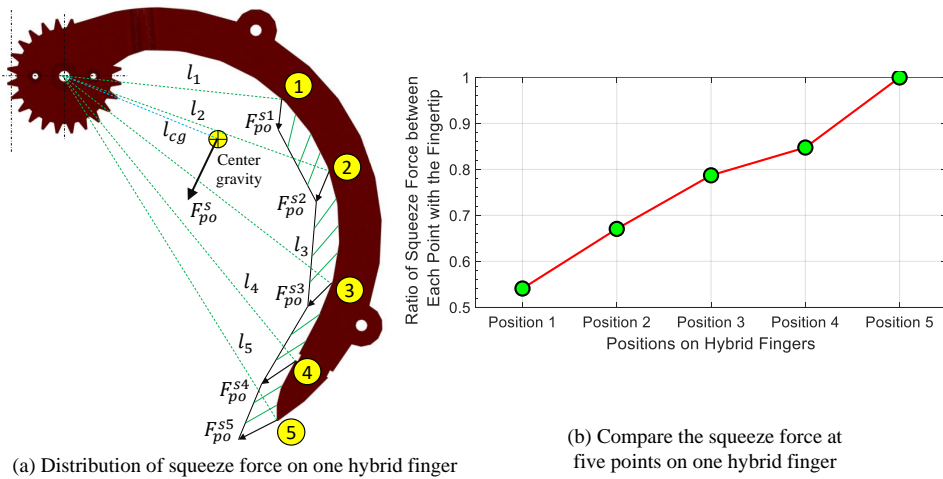(b) Compare the squeeze force at five points on one hybrid finger

Fig. 7. Estimating the distribution of the squeezing force generated on the hybrid robot finger. (a) Schematic illustration of the squeezing force at the center of gravity and at five key points on the hybrid robot finger. (b) Comparison of the ratio of the squeezing forces generated at five points on the hybrid finger to the force at the fingertip's point

where m_f, α, t are mass of the rotational finger, rotational angle and rotational time, respectively. Applying the real data in Table 2 to Eq. (4) we derive the force $F_{po}^s = 0.98$ N. Additionally, as shown in Fig. 7b, the force F_{po}^s was reduced from the fingertip point to the point 1. In other words, the ratios of squeezing forces at these points to the force at the fingertip are $F_{po}^{s1}/F_{po}^{s5}, F_{po}^{s2}/F_{po}^{s5}, F_{po}^{s3}/F_{po}^{s5}, F_{po}^{s4}/F_{po}^{s5} = 0.54$, 0.66, 0.79, 0.84. These ratios depend on the lengths $l_1, l_2, ..., l_5$.

Table 2. Main parameters of the object showcases

Parameters	Value
l_1	61.7 (mm)
l_2	76.5 (mm)
l_3	89.8 (mm)
l_4	96.7 (mm)
l_5	114.1 (mm)
l_{cg}	47.3 (mm)
m_f	117.7 (g)
α	110 (deg)
t	0.2 (s)

In both robot hands, the forces F_{po}^s reach a maximum value at the fingertip point, and in the case of soft robot hand this force is much greater than that in the case of the hybrid finger.

5.2. Grasping ability

As shown in Fig. 8, in the case of the hybrid hand, the average number of successfully grasped objects such as mixing sticks, toothbrushes, and tea packs was 7, 2.14 and 3.5 times higher, respectively, than that in the case of the soft finger. In this scenario, the hybrid hand can grasp, on average, 28.4, 22.8, and 24.6 items in one grasping time, whereas, the soft hand only 4.6, 10.4 and 7.6 items. Fig. 9 shows that the hybrid robot hand reaches maximum rates of remaining items for the mixing stick, toothbrush and tea pack of roughly 64.5, 8.3, and 29.7 %, and at the 4th trial, when grasping the toothbrush, the success rate reaches 100 %. In contrast, the remaining rates for these three objects in the case of soft robotic hand are in the range of 92.5÷96.3 %, 62.5÷45.8 %, and 71.4÷80 %, respectively. That is, the rate of successful grasping in the case of using the soft robot hand is much lower than that when using the hybrid one.
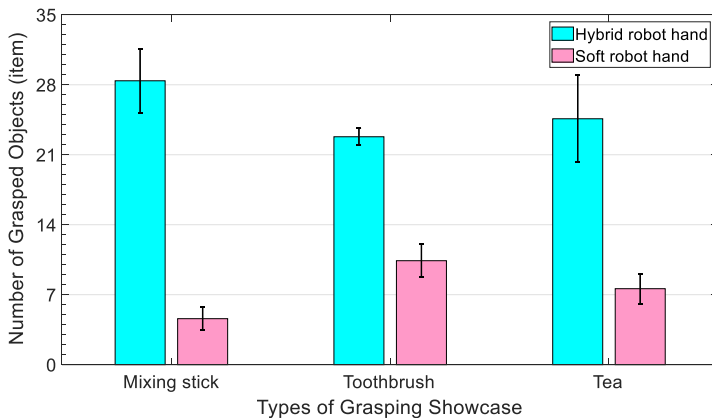
Fig. 8. Comparison of grasping ability between the hybrid and the soft robot hand based on the number grasped objects. In this scenario, blue and pink bars show the average numbers of grasped objects in the cases of hybrid and soft robot hands, respectively. Whiskers denote errors in different trials

For this experiment, the group of toothbrush was conducted such that both the soft and rigid robot fingers can grip them one time; meanwhile the robot hands can only grip a part of the total mixing stick and tea pack. Fig. 10 illustrated the grasping states for each kind of the group objects. The group objects were grasped and lifted in stable state between the hybrid finger (see Fig. 10a). In this scenario, the grasped objects almost were in the stable state inside the red-dash curves. After the robot hand moved up, just 1÷2 mixing stick and brushes fell down, while other grasped objects still lied on inside the robot fingers. In contrast, the soft robot hand initially grasped a large number of the toothbrushes and tea packs, but a huge part of them dropped after lifting up (see Fig. 10b). The grasped objects in the soft hand case did not achieve stable state, indeed, at further locations from the grasping interfaces,
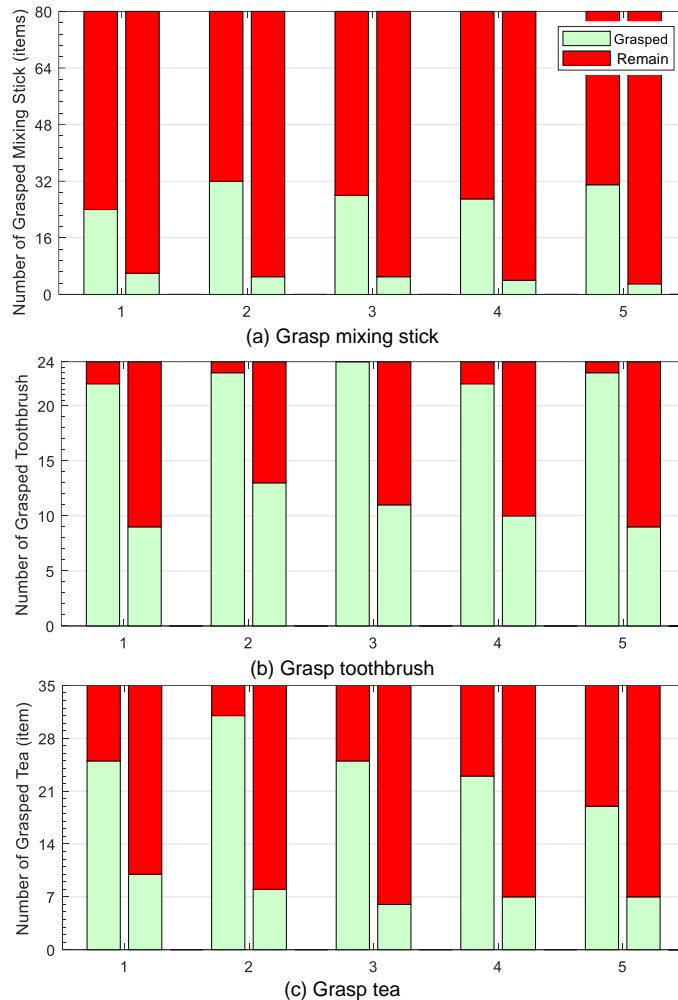
Fig. 9. Trials of grasping group objects with three showcases: mixing stick (a), toothbrush (b) and tea pack (c) conducted with the hybrid robot hand and the soft robot hand. The graph shows the ratio of successfully grasped objects in the total number of initial objects. In this figure, green and the red colors illustrate the number of objects successfully gripped and remaining kept after each trial, respectively. In addition, in each pair of comparison bars, the left and right bar show the statistical data for the hybrid and the soft robot hands, respectively

the more brushes and tea packs began vibrating and moving in random ways and then fell down quickly even though already increased the chamber pressure to the maximum value (40 kPa, see Fig. 6). That is, more rising the air pressure inside the soft fingers (means increased the force F_{po}^s in Eq. (3)) can increase the number of grasped objects but cannot assure enhance the stable state for grasping one group objects. Therefore, gripping the objects using the hybrid robot hand achieved more stable than that of using the soft robot hand.
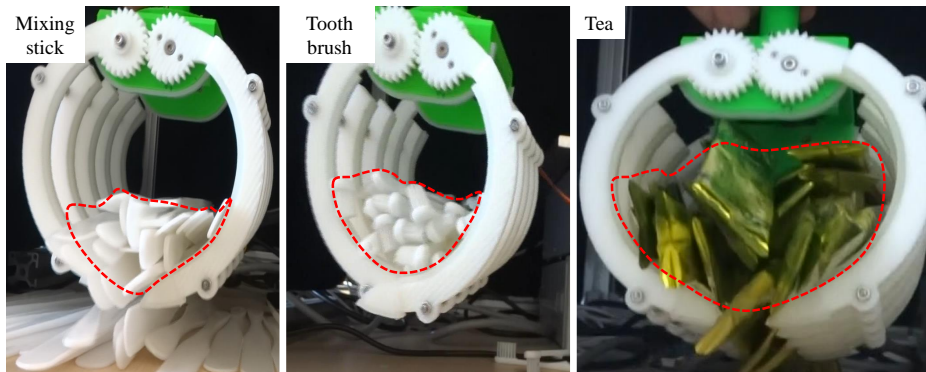
(a) Grasped performance in case using hybrid robot hand
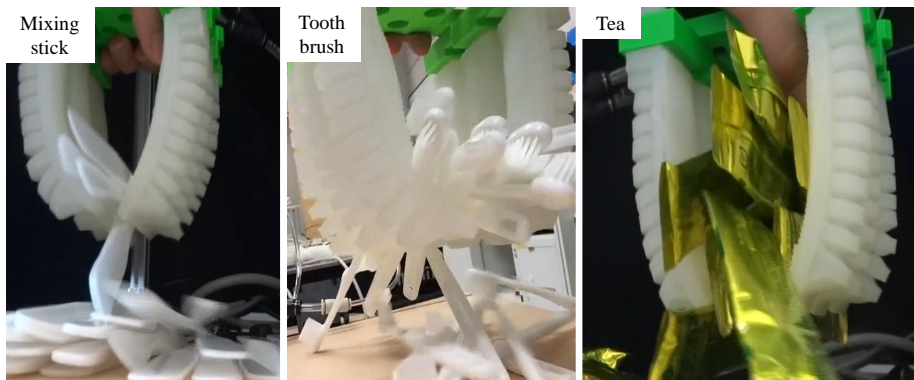
(b) Grasped performance in case using soft robot hand

Fig. 10. Comparison of grasping ability in stable conditions between the hybrid robot hand (a) and the soft robot hand (b). The red-dashed curves in (a) circumscribe the total cross-section area of the grasped objects in the case of the hybrid hand

Fig. 10 additionally illustrates that the cross-section areas of the grasped objects: the mixing stick, the tooth brush and the tea pack occupy about 30.8, 41.9, and 55.7 % respectively, of the total grasping space inside the hybrid robot hand. These percentages are higher than those in the soft hand case. That is, the hybrid robot hand performs better in gripping one group of objects per a grasping trial even though its grasping space is not occupied in 100%. In this situation, the hybrid robotic hand created the stable F_{po}^s, F_{po}^f determined in Eq. (3) along its length. Although the soft robot hand generated a sufficient F_{po}^s to grip the objects (even though it was greater than that in the hybrid case), this force was not stable along the length of the soft fingers during increasing the air pressure [23]. In fact, the soft materials and the structure of the Pneunet finger's bodies reduced the stability of the grasping. Such problems, hence, lead to unsatisfactory condition in Eq. (3), that is, obtaining the stable grasp by using the soft robot hand becomes more difficult. However, the soft robot hands can better absorb the reaction force, and increase

the force F_{po}^f in Eq. (3). To obtain such advantages, our rigid robot fingers were covered with the soft pads for creating a friendly interaction between the hybrid finger and the object. Hence, hybrid fingers had both stable and soft properties in handling the object showcases.

To validate the mathematical model presented in section 2, we apply Eqs. (1-3) to the showcases of the hybrid and soft robot hands in the experiments, as shown in Fig. 11. The squeezing forces F_{po}^s in the case of hybrid and soft robot hands are applied, respectively, to a place near the bottom and the top points of each of the contacted objects (see Fig. 11). These forces generate a different moment $M_{o,x}^s$ acting on the grasped objects. Indeed, in Fig. 11 (a and b) the objects tend to rotate in opposite directions. We assume that the connection between the grasped objects is sufficient for forming a soft beam. Hence, the group of objects in the case hybrid robot hand tends to bend up at the middle area, while this trend inverts in the case of the soft robot hand. That is, the objects are more unstable and more easily to fall down when grasping with the soft fingers even though a higher squeezing force F_{po}^s can be generated (see section 5.1).

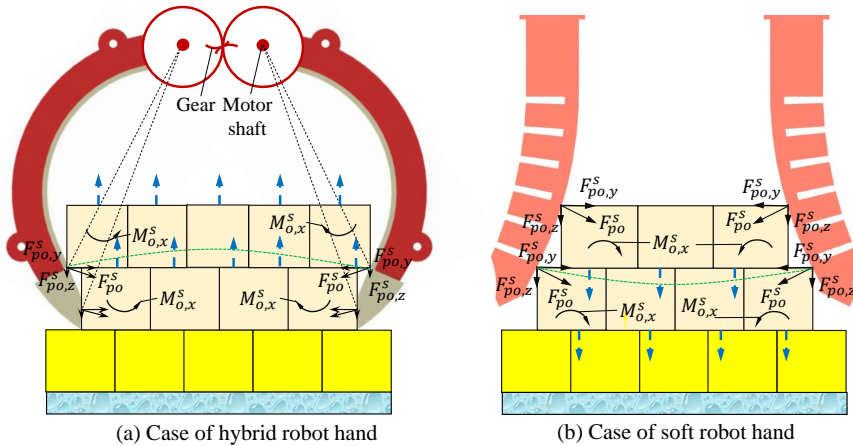(a) Case of hybrid robot hand   (b) Case of soft robot hand

Fig. 11. Schematic illustration of grasping one group objects by hybrid (a) and soft robot hands (b). In this figure, the squeezing force is divided into $F_{po,y}^s$ and $F_{po,z}^s$ in y, z directions. Additionally, $M_{o,x}^s$ is the moment of the grasped objects in x axis

6. Discussion

The experimental evidence proved that the hybrid robot hand can achieve better performance in grasping the group objects than the completely soft robot body. Also the experimental results showed a satisfactory agreement with the analytical model. There are several future works for continuing research presented in this paper:

- Optimization of the design of hybrid robot hand so that the occupied grasping space becomes larger. The robot fingers and the body should be softer to

become more adaptive to the universal objects. In addition, the robot hand should reduce the amount of failed objects after lifting.

- Evaluation of the theoretical model in various conditions, taking into account the properties of the objects, for predicting the grasping ability of the robot hand. Hence, it will be possible to refine the proposed analytical model in grasping the group objects. In addition, some control methods [24] may be necessary to apply.

7. Conclusions

Through evaluating the grasping ability for the group objects, the proposed design of the hybrid robot hand can ensure a higher number of grasped objects and guarantees a more stable grasp than that in the case of the soft robot hand. In addition, the experimental outcomes are in agreement with the proposed theoretical model. Therefore, the results obtained in this study provide a potential for expanding the research on manipulating group objects in the future.

Acknowledgements

References

[1] D. Rus and M.T. Tolley. Design, fabrication and control of soft robots. *Nature*, 521:467–475, 2015. doi: 10.1038/nature14543.

[2] S.N. Gorb. Biological attachment devices: exploring nature's diversity for biomimetics. *Philosophical Transactions of the Royal Society A: Mathematical, Physical and Engineering Sciences*, 366(1870):1557–1574, 2008. doi: 10.1098/rsta.2007.2172.

[3] S. Kim, M. Spenko, S. Trujillo, B. Heyneman, V. Mattoli, and M.R. Cutkosky. Whole body adhesion: hierarchical, directional and distributed control of adhesive forces for a climbing robot. *Proceedings 2007 IEEE International Conference on Robotics and Automation (ICRA)*, pages 1268–1273, 2007. doi: 10.1109/ROBOT.2007.363159.

[4] E. W. Hawkes, H. Jiang, D. L. Christensen, A. K. Han, and M. R. Cutkosky. Grasping without squeezing: Design and modeling of shear-activated grippers. *IEEE Transactions on Robotics*, 34(2):303–316, 2018. doi: 10.1109/TRO.2017.2776312.

[5] J. Shintake, S. Rosset, B. Schubert, D. Floreano, and H. Shea. Versatile soft grippers with intrinsic electroadhesion based on multifunctional polymer actuators. *Advanced Materials*, 28(2):231–238, 2016. doi: 10.1002/adma.201504264.

[6] B. Mazzolai, A. Mondini, F. Tramacere, G. Riccomi, A. Sadeghi, G. Giordano, E. Del Dottore, M. Scaccia, M. Zampato, and S. Carminati. Octopus-inspired soft arm with suction cups for enhanced grasping tasks in confined environments. *Advanced Intelligent Systems*, 1(6):1900041, 2019. doi: 10.1002/aisy.201900041.

[7] P.V. Nguyen and V.A. Ho. Grasping interface with wet adhesion and patterned morphology: Case of thin shell. *IEEE Robotics and Automation Letters*, 4(2):792–799, 2019. doi: 10.1109/LRA.2019.2893401.

[8] D.N. Nguyen, N.L. Ho, T.-P. Dao, and C.N. Le. Multi-objective optimization design for a sand crab-inspired compliant microgripper. *Microsystem Technologies*, 25, 2019. doi: 10.1007/s00542-019-04331-4.

[9] J. Hughes, U. Culha, F. Giardina, F. Guenther, A. Rosendo, and F. Iida. Soft manipulators and grippers: A review. *Frontiers in Robotics and AI*, 3:69, 2016. doi: 10.3389/frobt.2016.00069.

[10] Phoung H. Le, Thien P. Do, and Du B. Le. A soft pneumatic finger with different patterned profile. *International Journal of Mechanical Engineering and Robotics Research*, 10(10):577–582, 2021. doi: 10.18178/ijmerr.10.10.577-582.

[11] T.-P. Dao, N.L. Ho, T.T. Nguyen, H.G. Le, P.T. Thang, H.-T. Pham, H.-T. Do, M.-D. Tran, and T.T. Nguyen. Analysis and optimization of a micro-displacement sensor for compliant microgripper. *Microsystem Technologies*, 23:5375–5395, 2017. doi: 10.1007/s00542-017-3378-9.

[12] P.V. Nguyen, Q.K. Luu, Y. Takamura, and V.A. Ho. Wet adhesion of micro-patterned interfaces for stable grasping of deformable objects. *2020 IEEE/RSJ International Conference on Intelligent Robots and Systems (IROS)*, pages 9213–9219, 2020. doi: 10.1109/IROS45743.2020.9341095.

[13] M. Calisti, M. Giorelli, G. Levy, B. Mazzolai, B. Hochner, C. Laschi, and P. Dario. An octopus-bioinspired solution to movement and manipulation for soft robots. *Bioinspiration & Biomimetics*, 6(3):036002, 2011. doi: 10.1088/1748-3182/6/3/036002.

[14] K.C. Galloway, K.P. Becker, B. Phillips, J. Kirby, S. Licht, D. Tchernov, R.J. Wood, and D.F. Gruber. Soft robotic grippers for biological sampling on deep reefs. *Soft Robotics*, 3(1):23–33, 2016. doi: 10.1089/soro.2015.0019.

[15] 2F-85 and 2F-140 Grippers https://robotiq.com/products/2f85-140-adaptive-robot-gripper.

[16] Forestry Cranes https://marchesigru.com/en/forestry-cranes-2.

[17] H. Hyyti, V.V. Lehtola, and A. Visala. Forestry crane posture estimation with a two-dimensional laser scanner. *Journal of Field Robotics*, 35(7):1025–1049, 2018. doi: 10.1002/rob.21793.

[18] K.W. Allen. *Encyclopedia of Physical Science and Technology – Materials*. Elsevier, 2001.

[19] P.V. Nguyen, T.H. Bui, and V.A. Ho. Towards safely grasping group objects by hybrid robot hand. *2021 4th International Conference on Robotics, Control and Automation Engineering (RCAE)*, pages 389–393, 2021. doi: 10.1109/RCAE53607.2021.9638841.

[20] T.-L. Le, J.-C. Chen, F.-S. Hwu, and H.-B. Nguyen. Numerical study of the migration of a silicone plug inside a capillary tube subjected to an unsteady wall temperature gradient. *International Journal of Heat and Mass Transfer*, 97:439–449, 2016. doi: 10.1016/j.ijheatmasstransfer.2015.11.098.

[21] P.V. Nguyen and V.A. Ho. Wet adhesion of soft curved interfaces with micro pattern. *IEEE Robotics and Automation Letters*, 6(3):4273–4280, 2021. doi: 10.1109/LRA.2021.3067277.

[22] J. Gao, W.D. Luedtke, D. Gourdon, M. Ruths, J.N. Israelachvili, and U. Landman. Frictional forces and amontons' law: From the molecular to the macroscopic scale. *The Journal of Physical Chemistry B*, 108(11):3410–3425, 2004. doi: 10.1021/jp036362l.

[23] D. Maruthavanan, A. Seibel, and J. Schlattmann. Fluid-structure interaction modelling of a soft pneumatic actuator. *Actuators*, 10(7):163, 2021. doi: 10.3390/act10070163.

[24] D.X. Phu, V. Mien, P.H.T. Tu, N.P. Nguyen, and S.-B. Choi. A new optimal sliding mode controller with adjustable gains based on Bolza-Meyer criterion for vibration control. *Journal of Sound and Vibration*, 485:115542, 2020. doi: 10.1016/j.jsv.2020.115542.